

# Towards Class Imbalance in Federated Learning

**Lixu Wang**

Northwestern University

lixuwang2025@u.northwestern.edu

**Shichao Xu**

Northwestern University

shichaoxu2023@u.northwestern.edu

**Xiao Wang**

Northwestern University

wangxiao@cs.northwestern.edu

**Qi Zhu**

Northwestern University

qzhu@northwestern.edu

## Abstract

Federated learning (FL) is a promising approach for training decentralized data located on local client devices while improving efficiency and privacy. However, the distribution and quantity of the training data on the clients' side may lead to significant challenges such as data imbalance and non-IID (non-independent and identically distributed) data, which could greatly impact the performance of the common model. While much effort has been devoted to helping FL models converge when encountering non-IID data, the imbalance issue has not been sufficiently addressed. In particular, as FL training is executed by exchanging gradients in an encrypted form, the training data is not completely observable to either clients or server, and previous methods for data imbalance do not perform well for FL. Therefore, it is crucial to design new methods for detecting data imbalance in FL and mitigating its impact. In this work, we propose a monitoring scheme that can infer the composition proportion of training data for each FL round, and design a new loss function – **Ratio Loss** to mitigate the impact of the imbalance. Our experiments demonstrate the importance of detecting data imbalance and taking measures as early as possible in FL training, and the effectiveness of our method in mitigating the impact. Our method is shown to significantly outperform previous methods, while maintaining client privacy.

## 1 Introduction

The emergence of federated learning (FL) enables multiple devices to collaboratively learn a common model without the need to collect data directly from local devices. It reduces the resource consumption on the cloud and also enhances the client privacy. FL has seen promising applications in multiple domains, including mobile phones [1–3], wearable devices [4, 5], autonomous vehicles [6, 7], etc.

In standard FL, a random subset of clients will be selected in each iteration, who will upload their gradient updates to the central server. The server will then aggregate those updates and return the updated common model to all participants. During FL, one major challenge is that data owned by different clients comes from various sources and may contain their own preferences, and the resulting diversity may make the convergence of the global model challenging and slow. Moreover, the phenomenon of data imbalance happens frequently in practical scenarios, e.g., the number of patients diagnosed with different diseases varies greatly [8], and people have different preferences when typing with G-board [3] (a practical FL application proposed by Google). When a model encounters data imbalance, samples of *majority classes* account for a very large proportion of the overall training data, while those of *minority classes* account for much less. The direct impact of data imbalance is the reduction of classification accuracy on minority classes. In many practical cases, those minority classes play a much more important role beyond their proportion in data, e.g.,

wearable devices need to be more sensitive to abnormal heart rates than normal scenarios, and it is more important for G-board to predict SOS precisely than restaurant names.

In the literature, a number of approaches have been proposed to address data imbalance, e.g., applying various data sampling techniques [9, 10], using generative augmentation to make up for the lack of minority samples [11, 12], and integrating cost-sensitive thoughts into model training [13]. However, during FL, the communication between clients and the server is restricted to the gradients and the common model, and for privacy concern, it is preferable that the server does not require clients to upload additional information about their local data [14, 15]. Thus, it is infeasible to gather the information of all local data and conduct an aggregated analysis globally. This makes the vast majority of imbalance solutions not applicable to FL. There are several approaches that may be applied locally, without uploading data distribution to the server [16–18]. However, due to the mismatch between local data distributions and the global one, these approaches are not effective and may even impose negative side-effect on the global model. The work in [19] directly addresses data imbalance in FL, however, it requires clients to upload their local data distribution to the server, which may expose latent backdoor to attacks and lead to privacy leakage. Moreover, it requires placing a number of proxy server, which increases the FL complexity and incurs more computation overhead.

In this work, we address the data imbalance issue in FL and tackle the above challenges. We consider FL as a scheme that is always in training [20]. During FL, new data is constantly generated by the clients, and data imbalance could happen at any time. If such imbalance cannot be detected in time, it may poison the common model and deteriorate the FL result. Thus, to detect the imbalance in FL timely and accurately, we propose to design a monitor that constantly samples the data imbalance across different classes/labels during FL and alerts the administrator when to apply measures that can mitigate its negative impact. Moreover, we develop a new loss function **Ratio Loss** based on our monitoring method, and compare our approach to existing loss-based imbalance solutions based on **CrossEntropy Loss** and **Focal Loss** [21] (those loss functions are for general data imbalance problems, and we implement them under FL setting).

The basic workflow of our method is shown in Fig. 1. At round  $t + 1$ , the monitor downloads the global common model  $G_t$  of the last round and feeds samples of the auxiliary data to it. For each class, the monitor obtains corresponding gradient updates  $g_L$ . And by applying our method to compare these updates with  $G_{t+1}$ , our monitor can acquire the composition of training data at round  $t + 1$ . If data imbalance is detected, our method will try to mitigate its impact by applying the Ratio Loss function in FL.

**Our contributions.** More specifically, we made the following contributions in this work:

- Our approach monitors the composition of training data at each training round in a passive way. The monitor can be deployed at either the central server or a client device, and it will not incur significant computation overhead or reduce client privacy.
- Our works show the importance of detecting data imbalances as early as possible during FL and taking timely measures; otherwise, a greater price has to be paid at later training stages to mitigate the impact of imbalance.
- Our approach defines two types of imbalance in FL: **local imbalance** and **global imbalance** (details in Sec. 3.2), and addresses global imbalance based on our monitoring scheme and a new loss function (Ratio Loss). Our method significantly outperforms previous state-of-the-art methods while maintaining privacy for the clients.

## 2 Related Work

**Data Imbalance.** In supervised learning, models require labeled training data for updating their parameters. The imbalance of the training data (i.e., the variation of the number of samples for different classes/labels) occurs in many scenarios, e.g., image recognition for disease diagnosis [8], object detection in autonomous vehicles [21], resource exploration [22], etc. Such data imbalance may worsen the performance of the learning models, in particular decreasing the classification accuracy for minority classes [23]. Several works have designed new metrics [24–26] to quantify the model performance with data imbalance, rather than just considering the overall accuracy. Prior approaches to address data imbalance can be classified into three categories: data-level, algorithm-

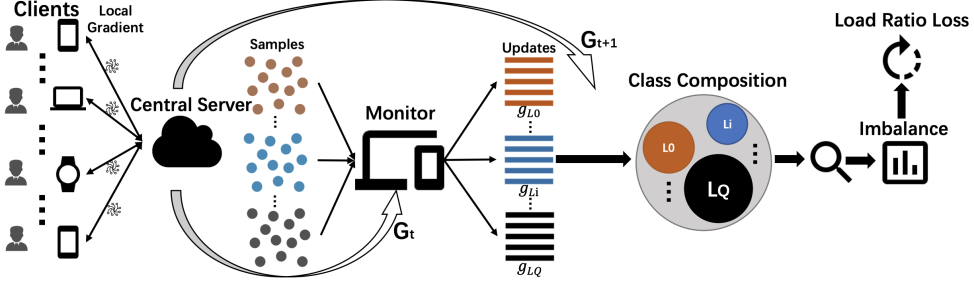


Figure 1: The monitor downloads the current global model  $G_t$ , and trains different labels on  $G_t$  to obtain corresponding updates  $\{g_{L1}, \dots, g_{LQ}\}$ . It then estimates the composition of training data by analyzing these updates with  $G_{t+1}$ . When detecting the data imbalance, the system loads the **Ratio Loss** in FL to mitigate its impact.

level, and hybrid methods. Data-level approaches leverage data re-sampling [27, 9, 28, 29, 10] and data augmentation [11, 12]. Algorithm-level approaches modify the training algorithm or the network structure, e.g., meta learning [30], model tuning [12], cost-sensitive learning [31, 16–18, 24], and changing the loss function [24, 13, 21]. Then, from the perspectives of both data and algorithm levels, hybrid methods emerge as a form of ensemble learning [32, 33].

As stated in Sec. 1, data-level methods cannot be applied in FL due to their violation of the privacy requirements. Some cost-sensitive approaches [31, 16–18] at the algorithm level need to analyze the distribution of training data, e.g., re-weighting the loss via inverse class frequency, and are not effective for FL due to the mismatch between local data distribution and the global one. Other cost-sensitive methods need specific information of minority classes, e.g., **MEF Loss** [24] regards minority classes as positive classes, and calculates false positive and false negative to generate a new loss form. Such requirement on prior knowledge is also difficult to acquire in FL. To address data imbalance in FL, we think that it is important to measure the imbalance according to the common model rather than depending on the knowledge of training data.

**Federated Learning.** Due to the heavy computation burden for training deep learning models, researchers have been exploring using multiple devices to learn a common model. There are many studies on organizing multiple devices for distributed learning, with both centralized [34–36] and decentralized [37, 38] approaches. Recently, more and more local client devices (e.g., mobile phones) can participate in model learning, with the advancement of their computation power. Under such circumstances, the training data on local devices is more personal and privacy-sensitive. In order to avoid privacy leakage, federated learning [39, 40, 20] has emerged as a promising solution, which enables a global model to be learned while keeping all training data on local devices. The privacy protection in the training is guaranteed by secure aggregation protocols [41] and differential privacy techniques [14, 15]. In general, with these technologies, neither local participants or central server of FL can observe the local gradient information during training. Despite of various types of inference attacks [42–45], inferring information of particular clients is still extremely difficult. Therefore, how to extract useful information from the global gradient after the central aggregation is interesting – and in this work, we focus on extracting such information for addressing data imbalance.

### 3 Our Method

#### 3.1 Definition and Background

Our problem is formulated on a multi-layer feed-forward neural network. Here we consider a classifier with output size equals to the number of classes  $Q$ . It is defined over a feature space  $\mathcal{X}$  and a label space  $\mathcal{Y} = \{1, \dots, Q\}$ . Without losing generality for our problem, we combine all the middle layers as a hidden layer  $HL$ . The feature vector and calibrated label for the  $j$ -th sample of class  $p$  is denoted as  $\mathcal{X}_j^{(p)}$  and  $c_j^{(p)}$ , respectively, where  $\mathcal{X}_j^{(p)} = (x_{j,1}^{(p)}, \dots, x_{j,r}^{(p)})$  and its corresponding output of  $HL$  is denoted as  $Y_j^{(p)} = (y_{j,1}^{(p)}, \dots, y_{j,s}^{(p)})$ . The inputs of the classifier and the  $HL$  contain  $r$  and  $s$  neurons, respectively. A function  $f : \{\mathcal{X} \Rightarrow \mathcal{S}\}$  maps  $\mathcal{X}$  to the output probability simplex  $\mathcal{S}$  of the network,

with  $f$  parameterizing over the hypothesis class  $\mathbb{W}$ , i.e., the overall weight of the neural network. Further, the link between the input layer and the  $HL$  is denoted as  $\mathcal{W} = (\mathcal{W}_{(1)}, \mathcal{W}_{(2)}, \dots, \mathcal{W}_{(s)})$ . The connection weight from the  $HL$  to the output layer is denoted as  $\mathcal{W} = (\mathcal{W}_{(1)}, \mathcal{W}_{(2)}, \dots, \mathcal{W}_{(Q)})$ . Finally, the weights of the network are denoted as  $\mathbb{W} = (\mathcal{W}, \mathcal{W})$ . At each training iteration, we apply backpropagation to compute the gradient of loss  $L(\mathbb{W})$  subject to the weights in  $\mathbb{W}$ . We use  $\mathbb{W}(m)$  to denote the weights in the  $m$ -th training iteration, and  $\lambda$  to denote the learning rate. We then have:

$$\mathbb{W}(m+1) = \mathbb{W}(m) - \lambda \nabla L(\mathbb{W}(m)) \quad (1)$$

We also leverage the following two theorems for two-class classifiers [46].

**Theorem 1:** If inputs over a period of time belong to a same class, the weight changes in the early stage of training have the same sign for all samples of the positive class and the opposite sign for all samples of the negative class.

**Theorem 2:** The expectations of gradient square for different classes have the following relation:

$$\varepsilon(\|\nabla L_p(\mathbb{W})\|^2) : \varepsilon(\|\nabla L_n(\mathbb{W})\|^2) \approx n_p^2 : n_n^2 \quad (2)$$

where  $n_p$  and  $n_n$  are the number of samples for the positive and negative class, respectively, and  $\varepsilon$  denotes the calculation of expectation values. The work in [46] also presents the following numeric results. For a particular class  $i$ , the coefficient before  $n_i^2$  is a function  $e : \{c^{(i)}\}$  parameterized over the calibrated label:

$$\varepsilon(\|\nabla L_i(\mathbb{W})\|^2) \approx e(c^{(i)}) n_i^2 \quad (i = 1, 2, \dots, C) \quad (3)$$

### 3.2 Monitoring Scheme

We define two types of data imbalance in FL: **local imbalance** and **global imbalance**. On every local client device  $j$ , the number of samples for each class  $i$ , denoted by  $N_i^j$ , may vary. The concept of local imbalance measures the extent of such variation on each client device. Specifically, we define the local imbalance  $\gamma_j$  for device  $j$  as the ratio between the sample number of the majority class on  $j$  and the sample number of the minority class on  $j$ , i.e.,  $\gamma_j = \max_i\{N_i^j\} / \min_i\{N_i^j\}$ , similar to the prevailing imbalance ratio measurement as in [47]. It is possible that  $\min_i\{N_i^j\} = 0$ , we regard this situation as the extreme imbalance. Then, from a global perspective, considering the aggregation of all the training data on local devices, we can measure the extent of global data imbalance  $\Gamma$  by defining it as the ratio between the total sample number of the majority class across all devices and that of the minority class, i.e.,  $\Gamma = \max_i\{\sum_j N_i^j\} / \min_i\{\sum_j N_i^j\}$ .

In general, the local imbalance on each device may be different from the global imbalance, and in practice such difference could be quite significant. We may even have the cases where a class is the majority class on certain local device but the minority class globally. To better quantify such mismatch between local and global imbalance, we use a vector  $v_j = [N_1^j, N_2^j, \dots, N_Q^j]$  to denote the composition of local data on device  $j$ , where  $Q$  is the number of classes; and we use a vector  $V = [\sum_j N_1^j, \sum_j N_2^j, \dots, \sum_j N_Q^j]$  to denote the composition of global data. We then use cosine similarity (CS) score to compare their similarity, i.e.,  $CS_j = (v_j \cdot V) / (\|v_j\| \|V\|)$ .

Because of the mismatch between local and global imbalance, simply adopting existing approaches at local devices is typically not effective and may even impose negative impact on global imbalance. To detect and mitigate the performance degradation caused by global imbalance, we develop a monitoring scheme to monitor the composition of training data during FL. First, we extend the **Theorem 2** to FL, and prove that the proportional relation between the expectation value of weight updates and the sample quantity still holds in FL.

**Proof of Proportional Relation.** The local training process of FL on a client device can be regarded as how a normal neural network learns from the training data. When a feed-forward network is optimized by modifying weights according to the gradient of training batch loss, for each sample within the batch, the feeding order is independent to the final batch gradient. Thus, the feeding process can be regarded as inputting all samples of the first class to the network, and when the feeding of the last class is over, the next class starts; although the feeding of batch could be out of order in practical training. With the order change, the feeding follows the assumption of **Theorem 1**, and we can remove the square symbol in Eq. (3).

In the setting of standard FL, the selected local gradients are aggregated by the FedAvg [20] algorithm:

$$\Delta \mathbb{W}_{t+1}^{Avg} = \frac{1}{K} \sum_{j=1}^K \Delta \mathbb{W}_{t+1}^j \Leftrightarrow \nabla L(\mathbb{W})_{t+1}^{Avg} = \frac{1}{K} \sum_{j=1}^K \nabla L(\mathbb{W})_{t+1}^j \quad (4)$$

where  $K$  represents the number of selected clients.

Eq. (4) depicts how FedAvg aggregates the uploaded gradient updates at iteration  $t + 1$ . We can then calculate the expectation value of the aggregated loss gradient:

$$\mathbb{E}(\nabla L(\mathbb{W})_{t+1}^{Avg}) = \mathbb{E}\left(\sum_{j=1}^K \frac{\nabla L(\mathbb{W})_{t+1}^j}{K}\right) = \sum_{j=1}^K \mathbb{E}\left(\frac{\nabla L(\mathbb{W})_{t+1}^j}{K}\right) \approx \frac{1}{K} \sum_{j=1}^K \sum_{i=1}^Q \sqrt{e(c^{(i,j)})} n_i^j \quad (5)$$

For a particular class  $\alpha$ , its samples owned by different clients can be calibrated as the same, and thus the  $e(c^{(\alpha,j)})$  of different clients are identical. Then, the corresponding expectation of aggregated gradient updates is:

$$\mathbb{E}_\alpha(\nabla L(\mathbb{W})_{t+1}^{Avg}) = \frac{\sqrt{e(c^{(\alpha)})}}{K} \sum_{j=1}^K n^{(\alpha,j)} = \frac{\sqrt{e(c^{(\alpha)})}}{K} \mathcal{N}_\alpha \quad (6)$$

where  $\mathcal{N}_\alpha$  is the number of overall samples for class  $\alpha$ . Now, we conclude that the proportional relation between the expected weight updates and the sample quantity still holds in FL.

Based on this relation, we develop our monitoring scheme as follows. In round  $t + 1$ , the monitor will feed samples of every class in the auxiliary data to the global common model from the last round, i.e.,  $G_t$ . It then obtains corresponding weight updates  $\{g_{L1}, \dots, g_{Li}, \dots, g_{LQ}\}$ , where each  $g_{Li}$  corresponds to the class  $i$ . In practice, we observe that not all weights get updated significantly – some of them increase little and thus easily get offset by other negative updates from feeding data of other classes. Accordingly, we design a filter to select the weights whose updating magnitudes are relatively large. Specifically, for class  $i$ , we extract its corresponding  $\Delta \mathcal{W}_{(i)}^{(1 \sim Q)}$  from  $\{g_{L1}, \dots, g_{Li}, \dots, g_{LQ}\}$ , and compute the ratio  $Ra_i$  of weight changes as follows:

$$Ra_i = \frac{(Q-1) \cdot \Delta \mathcal{W}_{(i)}^{(i)}}{\sum_{j=1}^Q (\Delta \mathcal{W}_{(i)}^{(j)}) - \Delta \mathcal{W}_{(i)}^{(i)}} \quad (7)$$

where  $\mathcal{W}_{(i)}$  is a weight vector whose size equals to the number of neurons at the hidden layer  $HL$ . We set a threshold  $T_{Ra}$  (in our experiments,  $T_{Ra} = 1.25$ ), and we select components of  $\mathcal{W}_{(i)}$  whose corresponding ratios  $Ra_i$  are larger than  $T_{Ra}$ .

Based on the proportional relation, we formulate the accumulation of weight changes under FedAvg:

$$\Delta \mathcal{W}_{(i)}^{(i)} \cdot \mathcal{N}_i + \left( \sum_{j=1}^K \sum_{i=1}^Q N_i^j - \mathcal{N}_i \right) \cdot \frac{\Delta \mathcal{W}_{(i)}^{(i)}}{Ra_i} = K \cdot (\mathcal{W}_{(i)}^{G_{t+1}} - \mathcal{W}_{(i)}^{G_t}) \quad (8)$$

where  $\mathcal{N}_i$  is the predicted sample quantity of class  $i$ ,  $K$  is the number of selected clients at the current round.  $\mathcal{W}_{(i)}^{G_t}$  and  $\mathcal{W}_{(i)}^{G_{t+1}}$  are link weights  $\mathcal{W}_{(i)}$  of the current and next global model  $G_t$  and  $G_{t+1}$ , respectively.  $\sum_{i=1}^Q N_i^j$  is the overall number of all data samples owned by client  $j$ , and we need clients to upload  $\sum_{i=1}^Q N_i^j$  to the server. This is the only information needed from clients in our monitoring scheme. Compared with other privacy-sensitive requirements, our requirement exposes little client information and should be acceptable for most security considerations. Now, except for  $\mathcal{N}_i$ , all values in Eq. (8) can be acquired by the monitor. We can then compute  $\mathcal{N}_i$  for each component of the filtered  $\mathcal{W}_{(i)}$ . There could still be some abnormal results, e.g., some  $\mathcal{N}_i$  could be smaller than 0 or larger than  $\sum_{j=1}^K \sum_{i=1}^Q N_i^j$ . We will remove those outliers and obtain the final result as the average of all calculated  $\mathcal{N}_i$ . After the computation for all classes, we can obtain the proportion vector of the current training round  $v_{pt} = [\mathcal{N}_1, \dots, \mathcal{N}_i, \dots, \mathcal{N}_Q]$ , an estimation of the global imbalance.

### 3.3 Ratio Loss based Mitigation

Once our monitor detects the data imbalance by checking  $v_{pt}$ , we will apply a mitigation strategy that is based on our design of the **Ratio Loss** function. The reasoning of this design is explained below.

As aforementioned, applying existing approaches locally will not be effective in mitigating the impact of global imbalance. Our method instead measures the global imbalance based on the current global common model. According to **Theorem 2**, weight updates are proportional to the quantity of samples for different classes, and the current network is built by accumulating such updates round by round. Due to the difference of feature space among classes, it seems more reasonable to use the contribution to gradient updates rather than just the numbers of data samples for demonstrating the imbalance problem in FL. In other words, after feeding some data to train the network, if weights of different nodes are updated similarly in terms of magnitude, we can regard the training as balanced, and vice versa. Because the layers before output nodes are shared by all classes, we restrict our interest on link weights between the  $HL$  and output nodes. Specifically, we consider the imbalance problem in FL as *the weight changes of different output nodes present noticeable magnitude gap when feeding samples of the corresponding class*.

We have also proven that the magnitude of weight updates for different classes will have significant difference if the current model is trained with data imbalance. The detailed proof is shown in the Supplementary Materials. Based on these observations, we propose to mitigate global imbalance by designing a new loss function – **Ratio Loss** (denoted as  $L_{RL}$ ). Specifically, we first consider the widely-used **CrossEntropy Loss** function for multi-class classifier (denoted as  $L_{CE}$ ):

$$L_{CE}(i, f) = - \sum_j^Q i \cdot \log(f_j) \quad (9)$$

where  $i$  is the ground-truth label and it is always the one-hot form in multi-class classifiers, while  $f_j$  denotes the probability results of different output nodes. In order to address the data imbalance, a common method is to introduce a weight vector  $\Pi = [\pi_1, \dots, \pi_Q]$ , then  $L_{CE}$  becomes balanced –  $\Pi \cdot L_{CE}$ . Usually,  $\pi$  is determined by the proportions of different classes for the overall training data. Intuitively, a larger proportion corresponds to a lower  $\pi$ , and vice versa.

As stated above, we use the noticeable differences of weight changes to evaluate the global imbalance. Taking the CrossEntropy Loss  $L_{CE}$  as the basic term, we define the Ratio Loss function  $L_{RL}$  as:

$$L_{RL} = -(\alpha + \beta \mathbb{R}) \cdot L_{CE} \quad (10)$$

where  $\alpha$  and  $\beta$  are two hyper-parameters. In our experiments, when  $\alpha = 1.0$  and  $\beta = 0.1$ , the mitigation results are the best (the experiment results on this can be found in the Supplementary Materials).  $\mathbb{R}$  is determined from the aforementioned  $\{g_{L1}, \dots, g_{Li}, \dots, g_{LQ}\}$ . After computing  $Ra_i$  of all output nodes as Sec. 3.2, we can compose  $\mathbb{R} = [Ra_1, \dots, Ra_i, \dots, Ra_Q]$ . Finally, in the local training, when a sample of class  $i$  is fed to the neural network, its corresponding loss is:

$$L_{RL}(i, f) = -(\alpha + \beta \cdot Ra_i) \sum_j^Q i \cdot \log(f_j) \quad (11)$$

We mitigate the impact of data imbalance by modifying the coefficient  $\pi$  before  $L_{CE}$ . Intuitively, when the input is a minority class, its corresponding  $Ra$  is relatively large, and then its contribution to the overall loss will increase, and vice versa.

## 4 Experimental Results

### 4.1 Experiment Setup

All experiments are conducted on a server running Ubuntu 18.04 LTS, equipped with a 2.10GHz CPU Intel Xeon(R) Gold 6130, 64GB RAM, and NVIDIA TITAN RTX GPU cards. We implement the deep learning mainly in the PyTorch learning framework. Our experiments follow the standard structure of federated learning [48], with some modifications for communication efficiency [20]. We choose three different datasets: MNIST, CIFAR10, and Fer2013 [49]. The former two are classical datasets in image classification, while Fer2013 relates to face recognition. For each dataset, we

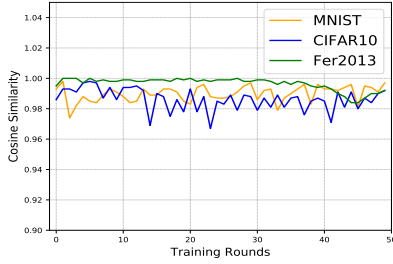


Figure 2: Similarity between our estimation of the global imbalance and the ground truth.

Metric	Stage	MNIST	CIFAR10	Fer2013
Ac.M %	End	31.64	03.28	06.99
	Middle	97.01	57.73	92.59
	Beginning	<b>97.81</b>	<b>68.27</b>	<b>99.67</b>
AUC	End	0.8816	0.6893	0.7648
	Middle	0.9896	0.7436	0.9463
	Beginning	<b>0.9903</b>	<b>0.7706</b>	<b>0.9970</b>

Table 1: Result comparison when data imbalance is detected at different stages of FL training.

utilize the following convolutional neural networks: LeNet5 for MNIST, a 5-layer CNN for CIFAR10, and Resnet18 [50] for Fer2013. The size of the local training batch is 32, and the learning rate is 0.001. We use the standard SGD optimizer to optimize the training process. The auxiliary data is a set of samples of different classes that is fed into the current learning model by the monitor. It can be acquired from the public data or generated by clients who are willing to share part of their data. Such auxiliary data can be utilized for a long time, unless the training data of the overall FL system changes significantly. Moreover, the required size of the auxiliary data is small. In our experiments, we use just 32 samples for each class, while the sample quantity of a client is more than 10000. Due to the small size of the auxiliary data, the deployment of the monitor does not incur significant computation overhead, and we indeed did not observe noticeable additional processing time during our experiments.

#### 4.2 Effectiveness of Monitoring Scheme

We first conduct a set of experiments to evaluate the effectiveness of our monitoring scheme. In these experiments, the central server randomly selects 20 clients from 100 participants during each round of the FL training, and each client trains its model for 10 local epochs. We observe from the experiments that training 30 global epochs can make the model on MNIST converge, 50 for CIFAR10, and 50 for Fer2013. For each client, first the number of classes they have locally is randomly determined as an integer between 1 and  $Q$ . Then, the specific classes are randomly chosen for each client, with equal sample quantity for each class. During FL, different client selections at each round lead to varying data compositions. As introduced in Sec. 3.2, our monitor computes a data proportion vector  $v_{pt} = [\mathcal{N}_1, \dots, \mathcal{N}_i, \dots, \mathcal{N}_Q]$  for each training round, which is an estimation of the global imbalance. We can compare it against the ground truth, defined as  $V$  in Sec. 3.2.

Fig. 2 shows the comparison between our estimated global imbalance ( $v_{pt}$ ) and the ground truth  $V$ , measured by a cosine similarity score. The closer it is to 1, the more accurate our estimation is. From the figure, we can observe that our estimation of the data composition is very close to the ground truth. Among four datasets, the average similarity score is above 0.98 and higher than 0.99 for most of the time. Such results demonstrate the effectiveness of our monitoring scheme and its broad applicability. We also carry out experiments with different numbers of clients, and we find that the similarity score gets even closer to 1 with the increase of client number. The detailed results can be found in the Supplementary Materials.

#### 4.3 Overall Comparison with Previous Methods

We then conduct experiments to evaluate the overall effectiveness of our method, with both monitoring and Ratio Loss based mitigation, and compare it with previous methods based on CrossEntropy Loss and Focal Loss (those methods are for general data imbalance, and we implement them under FL setting). We use the similar experiment setting as Sec. 4.2, except that we now explicitly explore different levels of global imbalance  $\Gamma$ , i.e., setting the ratio between the majority class and the minority class as 10 : 1, 20 : 1, 50 : 1, and 100 : 1, respectively. The evaluation metrics are the AUC score and the classification accuracy of minority classes (Ac.M).

First, we would like to demonstrate the importance of detecting the data imbalance as early as possible. Table 1 shows the different results when the global data imbalance ( $\Gamma = 100 : 1$ ) is detected at the

Data		MNIST				CIFAR10				Fer2013			
$\Gamma$		10:1	20:1	50:1	100:1	10:1	20:1	50:1	100:1	10:1	20:1	50:1	100:1
Ac.M %	$L_{CE}$	90.19	80.04	63.66	46.84	23.43	15.17	04.93	00.97	23.59	12.65	05.43	02.41
	$L_{FL}$	84.84	75.65	63.43	41.76	<b>26.40</b>	<b>17.77</b>	<b>06.47</b>	<b>01.57</b>	21.87	<b>12.86</b>	<b>05.56</b>	<b>03.01</b>
	$L_{RL}$	<b>92.05</b>	<b>81.70</b>	<b>74.51</b>	<b>56.50</b>	<b>29.77</b>	<b>19.17</b>	<b>06.77</b>	<b>03.03</b>	<b>25.55</b>	<b>13.34</b>	<b>06.46</b>	<b>02.95</b>
AUC	$L_{CE}$	0.9780	0.9526	0.9338	0.9056	0.6944	0.6777	0.6628	0.6578	0.7932	0.7574	0.7320	0.7275
	$L_{FL}$	0.9642	0.9485	0.9282	0.8927	0.6790	0.6691	0.6498	<b>0.6584</b>	0.7599	0.7337	0.7241	0.7184
	$L_{RL}$	<b>0.9815</b>	<b>0.9644</b>	<b>0.9531</b>	<b>0.9213</b>	<b>0.7197</b>	<b>0.7084</b>	<b>0.6844</b>	<b>0.6820</b>	<b>0.7962</b>	<b>0.7482</b>	<b>0.7372</b>	<b>0.7268</b>

Table 2: Comparison between our method ( $L_{RL}$ ) and previous methods based on CrossEntropy Loss ( $L_{CE}$ ) and Focal Loss ( $L_{FL}$ ) in federate learning, over three datasets and different levels of global imbalance.

beginning (10-th epoch out of a total of 50 epochs), middle (30-th epoch), or towards the end (45-th epoch) of FL training. We can see that earlier detection can greatly help improve the performance.

In Table 2, we demonstrate the comparison between our method with Ratio Loss ( $L_{RL}$ ) and the previous methods based on CrossEntropy Loss ( $L_{CE}$ ) and Focal Loss ( $L_{FL}$ ), over all three datasets and different levels of global data imbalance. We can see that our method can effectively mitigate the impact of data imbalance and outperforms the previous methods in almost all cases (except in one case, where for Fer2013 and 100 : 1 imbalance, the Ac.M of our method is slightly worse than that of Focal Loss). Our improvement is particularly significant for MNIST, where the absolute improvement of Ac.M ranges between 6%-15%, and for the imbalance level of 10 : 1 across all datasets, where the absolute improvement of Ac.M ranges between 3%-7%.

In order to further evaluate the effectiveness of our method, we compare it with the two previous methods in the regular training of neural networks *without* federated learning. Table 3 demonstrates that in these cases, our method still outperforms the other two in most scenarios. This shows the broader potential of our Ratio Loss function.

#### 4.4 Impact of Mismatch between Local and Global Imbalance

As stated in Sec. 3.2, the mismatch between local and global imbalance (measured by their CS score  $CS$ ) could have significant impact on the training performance. Here, we conduct a set of experiments to explore such impact. We adjust the mismatch level by setting different number of classes each client may have, i.e., from 2 to 5 out of a total number of 10 classes globally. Intuitively, the smaller the number, the less representative each client is with respect to the global training set, and hence the larger the mismatch. Fig. 3 shows the Ac.M of the three methods under different levels of mismatch for the CIFAR10 dataset with a global imbalance of 10 : 1 (more results for other datasets and global imbalance level can be found in the Supplement Materials). Note that the x-axis shows the average mismatch level between local and global imbalance, measured by the average of the CS score  $CS_j$  over  $j$  – the larger the number, the more similar the two imbalance measurements are and the less the mismatch. From the figure, we can observe that 1) larger mismatch between local and global impact will worsen the performance for all methods, and 2) our method constantly outperforms the other methods under all levels of mismatch.

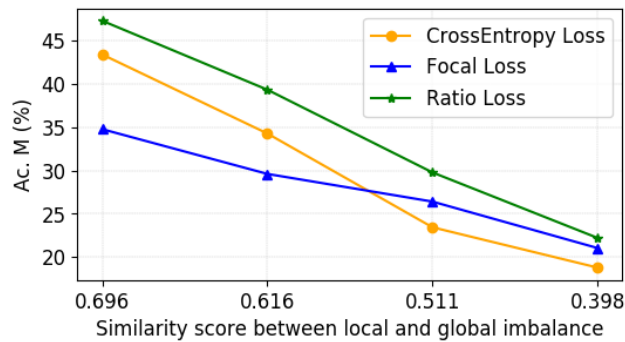


Figure 3: Comparison between our method with Ratio Loss and previous methods based on CrossEntropy Loss and Focal Loss under different levels of mismatch between local and global imbalance.

Data		MNIST				CIFAR10				Fer2013			
$\gamma$		10:1	20:1	50:1	100:1	10:1	20:1	50:1	100:1	10:1	20:1	50:1	100:1
Ac.M %	$L_{CE}$	90.14	85.86	75.64	51.20	17.93	11.84	01.53	00.47	10.95	04.70	01.85	00.91
	$L_{FL}$	<b>93.88</b>	<b>87.03</b>	<b>78.70</b>	<b>58.55</b>	<b>27.90</b>	<b>16.00</b>	<b>05.70</b>	<b>02.37</b>	<b>14.07</b>	<b>08.18</b>	<b>02.31</b>	<b>00.83</b>
	$L_{RL}$	<b>93.99</b>	<b>89.85</b>	<b>79.41</b>	<b>60.34</b>	<b>29.87</b>	<b>17.70</b>	<b>06.43</b>	<b>02.40</b>	<b>14.93</b>	<b>06.99</b>	<b>02.46</b>	<b>00.93</b>
AUC	$L_{CE}$	0.9793	0.9729	0.9543	0.9108	0.7354	0.7183	0.7078	0.7068	0.6975	0.6853	0.6752	0.6745
	$L_{FL}$	<b>0.9862</b>	<b>0.9739</b>	<b>0.9612</b>	<b>0.9151</b>	<b>0.7689</b>	<b>0.7530</b>	<b>0.7442</b>	<b>0.7318</b>	<b>0.7135</b>	<b>0.7029</b>	<b>0.6894</b>	<b>0.6893</b>
	$L_{RL}$	<b>0.9864</b>	<b>0.9801</b>	<b>0.9625</b>	<b>0.9306</b>	<b>0.7868</b>	<b>0.7712</b>	<b>0.7447</b>	<b>0.7416</b>	<b>0.7236</b>	<b>0.7049</b>	<b>0.6927</b>	<b>0.6905</b>

Table 3: Comparison between our method ( $L_{RL}$ ) and previous methods based on CrossEntropy Loss ( $L_{CE}$ ) and Focal Loss ( $L_{FL}$ ), when the models are not trained with federate learning.

## 5 Conclusion

We present a novel method to address the data imbalance issue in federate learning (FL). Our approach includes a monitoring scheme that can infer the composition of training data at every round of the FL and detect the possible global imbalance, and a new loss function (Ratio Loss) for mitigating the impact of global data imbalance. Experiments demonstrate that our method can significantly outperform previous methods in its accuracy of classifying minority classes, while maintaining the privacy for clients (with the total local sample quantities as the only information required).

## 6 Supplementary Material

### 6.1 Weight Update Difference Caused by Data Imbalance

In Section 3.3 of the paper, we stated that “the magnitude of weight updates for different classes will have significant difference if the current model is trained with data imbalance”, which led to the design of our **Ratio Loss** function. Here we will provide more detailed reasoning on this point, to explain the magnitude difference of weight updates among classes when the classifier is trained with imbalanced data. The symbols we use here follow the same notations in the main body of the paper. To help illustrate our idea, we consider a network structure as shown in Fig. 4.

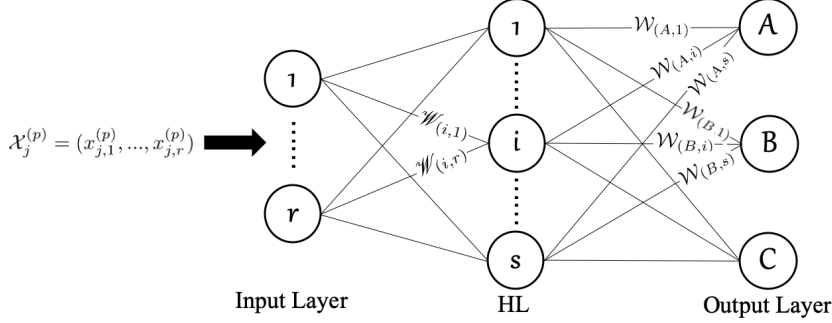


Figure 4: The structure of a multi-class feed-forward network.

In FL training, all weight changes are calculated as a product of the error signal for a node and the output of its former node [46, 24]. The weight update for each component in  $\mathcal{W}_{(p)}$  with respect to the  $(j, p)$ -th sample is given by :

$$\Delta \mathcal{W}_{(p,i)}^{(j,p)} = \lambda \underbrace{[(c_j^{(p)} - f_j^{(p)}) f_j^{(p)} (1 - f_j^{(p)})]}_{\text{Error signal of node}} y_{j,i}^{(p)} \quad (i = 1, 2, \dots, s) \quad (12)$$

Take an imbalanced scenario as an example. Assume that there is a 3-class (A, B, C) classifier as Fig. 4 shows, and class A is the majority class while class B is the minority one. The feeding features and output results of the network layers are non-negative under different activation functions (e.g., Sigmoid, ReLu), and the computation result of the  $p$ -th output neuron is a product between  $Y_j^{(p)}$  and  $\mathcal{W}_{(p)}$ . After inputting part of the dataset to train the network, if we feed a sample of class A to the network, the probability results of node A is much higher than that of node B [21], and thus this sample will be classified into class A. For nodes A and B, the output vector of the hidden layer  $HL$  is the same. What makes the difference between probability results is the difference between  $\mathcal{W}_{(A)}$  and  $\mathcal{W}_{(B)}$ . We can thus conclude:

$$f_A^{(A)} \gg f_B^{(A)} \Rightarrow \mathcal{W}_{(A)} \gg \mathcal{W}_{(B)} \quad (13)$$

Now let us analyze the magnitude difference of weight changes for nodes A and B when the network is first fed with a sample of class C. For node A, we can transfer the classification task into a two-class problem, and regard class A as the positive label and class C as the negative. Moreover, because the training of the current model has not received any contribution from class C, class A can be regarded as the majority class. Similar analysis can be applied to node B. When computing the probability results of nodes A and B, the results of the former layers ( $Y^{(C)}$ ) are identical. Combined with Eq. (13), the relation between probability results can be obtained as:

$$f_A^{(C)} = Y^{(C)} \mathcal{W}_{(A)} \gg f_B^{(C)} = Y^{(C)} \mathcal{W}_{(B)} \quad (14)$$

Based on Eq. (12), we can determine that the signs of weight change  $\Delta \mathcal{W}^{(C)}$  for both nodes A and B are negative. In addition, since nodes A and B are not the corresponding output nodes of class C, the probability results of these two nodes are not very high. Furthermore, with the relation given by Eq. (14), the probability output of node B is close to zero. For the magnitude of weight updates

given by Eq. (12), the second term  $y_{j,i}^{(p)}$  of different output nodes is the same, and thus the difference between the *Error signal of node* is responsible for the different degrees of weight change. When there is a large error ( $|c_j^{(p)} - f_j^{(p)}| \rightarrow 1$ ), the output probability is very high or very low ( $f_j^{(p)} \rightarrow 0$  or  $f_j^{(p)} \rightarrow 1$ ). In either case, one of the two terms,  $f_j^{(p)}$  or  $(1 - f_j^{(p)})$ , will remain relatively small. Because of this, the magnitude of weight updates will be very small accordingly.

Considering the analysis above, we can infer that when fed with a sample of class C, the magnitude of the *Error signal* for node B is very small and much smaller than that of node A:

$$|\Delta\mathcal{W}_{(A)}^{(C)}| \gg |\Delta\mathcal{W}_{(B)}^{(C)}| \quad (15)$$

If the current model is fed with samples of class A or B, weight  $\mathcal{W}$  of the corresponding output node will change. In this case, we consider the mean value of link weights for a single node, e.g., the average value of  $\Delta\mathcal{W}_{(A)} = [\Delta\mathcal{W}_{(A,1)}, \dots, \Delta\mathcal{W}_{(A,s)}]$  (as the notations in Fig. 4) when inputting the samples of class A. Under such circumstances, the output results of the hidden layer  $HL$  can be written as :

$$y_i^{(A)} = \mathcal{X}^{(A)}\mathcal{W}_{(i)} \quad (i = 1, 2, \dots, s) \quad (16)$$

Here,  $\mathcal{W}_{(i)}$  is a weight vector  $[\mathcal{W}_{(i,1)}, \dots, \mathcal{W}_{(i,r)}]$ . With Eq. (12), we can compute the mean of  $\Delta\mathcal{W}_A^{(A)}$ :

$$\frac{1}{s} \sum_{i=1}^s \Delta\mathcal{W}_{(A,i)}^{(A)} = \frac{\lambda\mathcal{X}^{(A)}}{s} [(c^{(A)} - f^{(A)})f^{(A)}(1 - f^{(A)})] \sum_{i=1}^s \mathcal{W}_{(i)} \quad (17)$$

Eq. (17) can be similarly applied to the weight changes of node B when the current network is fed with samples of class B. In either case, the  $\mathcal{W}_{(i)}$  in Eq. (17) is the same. Because class A is the majority class, the corresponding probability results are higher than that of class B [21]. Thus, we can conclude that:

$$[(c^{(A)} - f^{(A)})f^{(A)}(1 - f^{(A)})] \ll [(c^{(B)} - f^{(B)})f^{(B)}(1 - f^{(B)})] \quad (18)$$

Note that the magnitude of weight changes also depends on the size of inputting feature vectors of different classes, i.e.,  $|\mathcal{X}^{(p)}|$ . If we assume that  $|\mathcal{X}^{(A)}| = |\mathcal{X}^{(B)}|$ , then the relation of weight changes in different cases can be determined:

$$|\frac{1}{s} \sum_{i=1}^s \Delta\mathcal{W}_{(A,i)}^{(A)}| \ll |\frac{1}{s} \sum_{i=1}^s \Delta\mathcal{W}_{(B,i)}^{(B)}| \quad (19)$$

This shows that the weight updates of different classes can be significantly different if the model is trained with data imbalance, which motivates our design of the **Ratio Loss** function, as explained in the main body of the paper.

## 6.2 Additional Experimental Results

**Monitoring Scheme under Different Number of Selected Clients.** To further evaluate the effectiveness of our monitoring scheme, we carry out experiments with different number of participating clients at each ground on CIFAR10. For experiment setting, we set the overall number of clients to 1000, and randomly select 50, 100, 200 of them at each round, respectively, to upload their gradient updates. The results are shown in Fig. 5. We can see that with the increase of the selected client number, the similarity score between our estimation of the global imbalance and the ground truth becomes closer to 1, which helps further improve the performance of our approach.

**Hyper-parameters of Ratio Loss.** As stated in Section 3.3, the hyper-parameters  $\alpha$  and  $\beta$  in the Ratio Loss function are set to 1.0 and 0.1, respectively, in our experiments reported in Section 4. This is based on our calibration experiments on MNIST, as shown in Tables 4 and 5. The calibration experiments have the same setting as in Section 4.3, with the global imbalance ratio set as  $\Gamma = 50 : 1$ .

**Impact of Mismatch between Local and Global Imbalance (Additional Results).** In Section 4.4, we demonstrate the impact of the mismatch between local imbalance and global imbalance. Here we report more experimental results on this aspect, as shown in Table 6 for MNIST, Table 7 for more



Figure 5: Similarity score between our estimation of the global imbalance and the ground truth on CIFAR10, under different number of selected clients at each round.

$\alpha$	0.25	0.50	0.75	<b>1.00</b>	1.25	1.50	1.75	2.00	3.00	5.00
<b>AC.M %</b>	77.31	80.68	78.56	<b>82.52</b>	81.82	81.06	75.82	80.64	75.05	41.12
<b>AUC</b>	0.9579	0.9588	0.9608	<b>0.9692</b>	0.9663	0.9650	0.9562	0.9642	0.9519	0.8906

Table 4: Performance comparison under different  $\alpha$  values ( $\beta = 0.10$ , global imbalance  $\Gamma = 50 : 1$ ).

$\beta$	0.02	0.04	0.06	0.08	<b>0.10</b>	0.12	0.15	0.20	0.30
<b>AC.M %</b>	80.44	76.84	78.66	79.41	<b>82.52</b>	82.34	80.85	79.65	74.40
<b>AUC</b>	0.9641	0.9575	0.9608	0.9626	<b>0.9692</b>	0.9675	0.9645	0.9604	0.9496

Table 5: Performance comparison under different  $\beta$  values ( $\alpha = 1.00$ , global imbalance  $\Gamma = 50 : 1$ ).

experiments of CIFAR10, and Table 8 for Fer2013. Across all of these experiments, our approach with the Ratio Loss function  $L_{RL}$  performs the best, with respect to the improvement on AUC score and accuracy on minority classes.

**Evaluation of MFE Loss based Method under Our Monitoring Scheme.** We also implemented **MFE Loss** [24] in FL, and conducted experiments to evaluate the effectiveness of using our monitoring scheme with MFE Loss. As MFE Loss ( $L_{MFE}$ ) is based on **MSE Loss** ( $L_{MSE}$ ), we regard  $L_{MSE}$  as the baseline.

First of all, as stated in the main body of the paper (Section 2), using MFE Loss  $L_{MFE}$  requires knowing what minority classes specifically are. In FL, such information is difficult to acquire globally, and the standard method based on  $L_{MFE}$  can only analyze the local data of each client. However, our monitoring scheme is able to estimate the global imbalance accurately, which can provide the MFE Loss based method with the global information it needs.

Table 9 shows the comparison between the baseline method based on MSE Loss ( $L_{MSE}$ ), the standard MFE Loss based method that can only analyze local data of each client in FL setting (denoted as  $L_{MFE-L}$ ), and our improvement of the MFE Loss based method with our monitoring scheme that provides the global imbalance information (denoted as  $L_{MFE-G}$ ). In the experiments, the global imbalance ratio  $\Gamma = 20 : 1$ . From the results, we can clearly see that knowing the global imbalance information from our monitoring scheme can drastically improve the performance of the MFE Loss based method. Without such information, the standard MFE Loss based method cannot mitigate the impact of global data imbalance, and has similar performance as the baseline. We also notice that combining our monitoring scheme with MFE Loss may provide better results than Ratio Loss in some cases (e.g., MNIST) but worse ones in other cases (e.g., CIFAR10). We will investigate this further in our future work.

## Source Code

The source code of our work can be found in [https://github.com/balanced-f1/Make\\_FL\\_More\\_Balanced](https://github.com/balanced-f1/Make_FL_More_Balanced).

MNIST		CS=0.6960				CS=0.6158				CS=0.3984			
$\Gamma$		10:1	20:1	50:1	100:1	10:1	20:1	50:1	100:1	10:1	20:1	50:1	100:1
Ac.M %	$L_{CE}$	90.97	86.59	75.43	64.62	93.09	86.87	78.57	54.82	82.78	73.41	50.12	28.93
	$L_{FL}$	<b>92.41</b>	86.44	73.46	63.91	90.55	84.44	68.82	<b>56.18</b>	71.89	58.80	49.16	26.07
	$L_{RL}$	<b>93.02</b>	<b>87.41</b>	<b>76.79</b>	<b>65.18</b>	<b>93.61</b>	<b>88.13</b>	<b>81.27</b>	<b>64.58</b>	<b>85.54</b>	<b>81.41</b>	<b>57.95</b>	<b>38.48</b>
AUC	$L_{CE}$	0.9817	0.9724	0.9569	0.9356	0.9842	0.9692	0.9606	0.9202	0.9588	0.9434	0.9034	0.8630
	$L_{FL}$	<b>0.9821</b>	<b>0.9725</b>	0.9517	0.9346	0.9765	0.9660	0.9412	0.9202	0.9339	0.9119	0.8918	0.8534
	$L_{RL}$	<b>0.9859</b>	<b>0.9763</b>	<b>0.9591</b>	<b>0.9393</b>	<b>0.9850</b>	<b>0.9763</b>	<b>0.9657</b>	<b>0.9366</b>	<b>0.9678</b>	<b>0.9518</b>	<b>0.9101</b>	<b>0.8899</b>

Table 6: Comparison between our method based on Ratio Loss ( $L_{RL}$ ) and previous methods based on CrossEntropy Loss ( $L_{CE}$ ) and Focal Loss ( $L_{FL}$ ) in FL, over MNIST, under different levels of global imbalance (from 10 : 1 to 100 : 1) and various levels of mismatch between local and global imbalance (measured by the similarity score  $CS$ ).

CIFAR10		CS=0.6960				CS=0.6158				CS=0.3984			
$\Gamma$		10:1	20:1	50:1	100:1	10:1	20:1	50:1	100:1	10:1	20:1	50:1	100:1
AC.M %	$L_{CE}$	43.40	28.50	13.10	05.40	34.27	23.87	08.67	03.10	18.77	01.70	00.40	00.13
	$L_{FL}$	34.77	24.93	11.40	05.10	29.60	19.43	<b>09.07</b>	<b>03.47</b>	<b>21.03</b>	<b>12.13</b>	<b>02.37</b>	<b>00.80</b>
	$L_{RL}$	<b>47.30</b>	<b>31.57</b>	<b>15.77</b>	<b>05.74</b>	<b>39.33</b>	<b>25.03</b>	<b>06.77</b>	<b>03.90</b>	<b>22.20</b>	<b>05.10</b>	<b>03.17</b>	<b>02.40</b>
AUC	$L_{CE}$	0.7793	0.7553	0.7338	0.7215	0.7421	0.7257	0.7069	0.6957	0.6106	0.6025	0.6185	0.6147
	$L_{FL}$	0.7368	0.7217	0.7046	0.6927	0.7086	0.6923	0.6782	0.6688	<b>0.6429</b>	<b>0.6353</b>	<b>0.6275</b>	<b>0.6179</b>
	$L_{RL}$	<b>0.7985</b>	<b>0.7735</b>	<b>0.7515</b>	<b>0.7345</b>	<b>0.7661</b>	<b>0.7438</b>	<b>0.6844</b>	<b>0.7062</b>	<b>0.6221</b>	<b>0.6268</b>	<b>0.6193</b>	<b>0.6110</b>

Table 7: Comparison between our method based on Ratio Loss ( $L_{RL}$ ) and previous methods based on CrossEntropy Loss ( $L_{CE}$ ) and Focal Loss ( $L_{FL}$ ) in FL, over CIFAR10, under different levels of global imbalance (from 10 : 1 to 100 : 1) and various levels of mismatch between local and global imbalance (measured by the similarity score  $CS$ ).

Fer2013		CS=0.9343				CS=0.8489				CS=0.7411			
$\Gamma$		10:1	20:1	50:1	100:1	10:1	20:1	50:1	100:1	10:1	20:1	50:1	100:1
AC.M %	$L_{CE}$	63.62	42.18	19.13	10.57	55.72	35.54	16.05	08.02	42.68	25.67	11.01	04.76
	$L_{FL}$	61.74	40.38	18.99	08.95	53.95	31.63	14.05	06.96	41.63	24.68	09.16	04.36
	$L_{RL}$	<b>63.96</b>	<b>42.93</b>	<b>20.00</b>	<b>10.81</b>	<b>56.20</b>	<b>36.39</b>	<b>15.59</b>	<b>08.08</b>	<b>43.23</b>	<b>25.80</b>	<b>11.86</b>	<b>05.21</b>
AUC	$L_{CE}$	0.8983	0.8414	0.7848	0.7620	0.8756	0.8229	0.7746	0.7556	0.8413	0.7977	0.7619	0.7467
	$L_{FL}$	0.8929	0.8368	0.7848	0.7576	0.8721	0.8141	0.7698	0.7526	0.8390	0.7961	0.7575	0.7456
	$L_{RL}$	<b>0.8989</b>	<b>0.8428</b>	<b>0.7856</b>	<b>0.7628</b>	<b>0.8770</b>	<b>0.8252</b>	<b>0.7759</b>	<b>0.7622</b>	<b>0.8423</b>	<b>0.7988</b>	<b>0.7626</b>	<b>0.7475</b>

Table 8: Comparison between our method based on Ratio Loss ( $L_{RL}$ ) and previous methods based on CrossEntropy Loss ( $L_{CE}$ ) and Focal Loss ( $L_{FL}$ ) in FL, over Fer2013, under different levels of global imbalance (from 10 : 1 to 100 : 1) and various levels of mismatch between local and global imbalance (measured by the similarity score  $CS$ ).

Data		MNIST				CIFAR10					
CS		0.6960	0.6158	0.5111	0.6960	0.6158	0.5111	0.6960	0.6158	0.5111	0.6960
Ac.M %	$L_{MSE}$	00.00	00.00	00.00	03.00	00.30	00.20	00.00	00.00	00.00	00.00
	$L_{MFE} - L$	05.01	00.00	00.00	01.00	00.10	00.00	00.00	00.00	00.00	00.00
	$L_{MFE} - G$	98.29	96.15	90.77	19.57	15.33	09.87	00.00	00.00	00.00	00.00
AUC	$L_{MSE}$	0.8143	0.8104	0.8022	0.6609	0.6459	0.6270	0.0000	0.0000	0.0000	0.0000
	$L_{MFE} - L$	0.8228	0.8106	0.8025	0.6600	0.6421	0.6220	0.0000	0.0000	0.0000	0.0000
	$L_{MFE} - G$	0.9823	0.9789	0.9641	0.7076	0.6779	0.6351	0.0000	0.0000	0.0000	0.0000

Table 9: Comparison between the baseline method based on **MSE Loss**, the standard **MFE Loss** based method with only local knowledge in FL setting ( $L_{MFE}-L$ ), and our improved **MFE Loss** based method with global knowledge from our monitoring scheme ( $L_{MFE}-G$ ), over MNIST and CIFAR10, with global imbalance ratio  $\Gamma = 20 : 1$  and under different levels of mismatch between local and global imbalance (measured by  $CS$ ). We can see the significant improvement from using our monitoring scheme to obtain global imbalance information and use it in the MFE Loss based method.

## Broader Impact

Federated learning (FL) is proposed with two goals in mind: 1) utilize the distributed computation resources efficiently, and 2) enhancing data privacy protection at the client devices. There have been a number of FL applications in domains such as healthcare, transportation, and economy. Unlike standard machine learning techniques, FL-based applications run on local client devices, e.g., wearable smartwatches, autonomous vehicles, or digital bank accounts. The data collected at the clients in FL tend to be quite diverse. Moreover, due to the privacy consideration, participants in FL are not required to share their local data and just need to upload the gradients when they are selected. Therefore, the problems of diverse data distributions and sample imbalance among clients are often more serious in FL than centralized schemes.

In this work, we present a novel method to address the data imbalance issue in FL. Our method can be beneficial in a variety of scenarios:

- With our method, the system administrator can assess whether the learning process has encountered data imbalance in a timely manner, and if so, take measurements to mitigate its impact.
- Our method can help detect the intrusion from backdoor and poisoning attacks. Such attacks need to guide the model to their target directions by enhancing part of the weight updates while diminishing other weight changes. By monitoring the training round by round, the system can detect the abnormal changes in weight updates and the possibility of malicious attacks.
- The inferred information from our method can provide useful statistics without the collection of raw data, e.g., the government can infer the morbidity or infectivity of particular diseases when building an online disease diagnosis system among all hospitals.

However, note that if the monitor is compromised by malicious clients, there could be several risks: 1) attackers can identify the classes that may be easily attacked, e.g., by placing backdoor on majority classes to avoid the detection that is based on measuring the abnormal gradient increase; 2) attackers can obtain unfair competitive advantage, e.g., when there is a commodity registration system trained with FL, a malicious market can obtain the information of supply and demand for certain products from the inference in monitoring and adjust their price accordingly; and 3) attackers may use minority classes to identify particular clients, e.g., attackers can learn how many VIP clients participate in the training and when to participate in a chain sports clubs where there are some activities exclusively for the VIPs.

Our method includes a monitoring scheme and a new loss function (Ratio Loss) for mitigating the impact of data imbalance in FL. The Ratio Loss function  $L_{RL}$  can be applied in FL while maintaining privacy for clients (the vast majority of existing data imbalance solutions cannot). Our experiments demonstrate the advantage of this new loss function in mitigating data imbalance for FL, when compared with the popular Focal Loss and CrossEntropy Loss functions (Table 2 and Fig. 3). Moreover, the experimental results also demonstrate its effectiveness for standard neural network training without FL (Table 3), which shows its potential for other data imbalance problems.

## References

- [1] Davide Anguita, Alessandro Ghio, Luca Oneto, Xavier Parra, and Jorge Luis Reyes-Ortiz. A public domain dataset for human activity recognition using smartphones. In *Esann*, 2013.
- [2] Andrew Hard, Kanishka Rao, Rajiv Mathews, Fran oise Beaufays, Sean Augenstein, Hubert Eichner, Chlo  Kiddon, and Daniel Ramage. Federated learning for mobile keyboard prediction. *arXiv preprint arXiv:1811.03604*, 2018.
- [3] Swaroop Ramaswamy, Rajiv Mathews, Kanishka Rao, and Fran oise Beaufays. Federated learning for emoji prediction in a mobile keyboard. *arXiv preprint arXiv:1906.04329*, 2019.
- [4] Alexandros Pantelopoulos and Nikolaos G Bourbakis. A survey on wearable sensor-based systems for health monitoring and prognosis. *IEEE Transactions on Systems, Man, and Cybernetics, Part C (Applications and Reviews)*, 40(1):1–12, 2009.
- [5] Thien Duc Nguyen, Samuel Marchal, Markus Miettinen, Hossein Fereidooni, N Asokan, and Ahmad-Reza Sadeghi. Di IoT: A Federated Self-learning Anomaly Detection System for IoT. *arXiv preprint arXiv:1804.07474*, 2018.

- [6] Sumudu Samarakoon, Mehdi Bennis, Walid Saad, and Merouane Debbah. Distributed federated learning for ultra-reliable low-latency vehicular communications. *arXiv preprint arXiv:1807.08127*, 2018.
- [7] Sumudu Samarakoon, Mehdi Bennis, Walid Saad, and Merouane Debbah. Federated learning for ultra-reliable low-latency v2v communications. In *2018 IEEE Global Communications Conference (GLOBECOM)*, pages 1–7. IEEE, 2018.
- [8] R Bharat Rao, Sriram Krishnan, and Radu Stefan Niculescu. Data mining for improved cardiac care. *ACM SIGKDD Explorations Newsletter*, 8(1):3–10, 2006.
- [9] Inderjeet Mani and I Zhang. knn approach to unbalanced data distributions: a case study involving information extraction. In *Proceedings of workshop on learning from imbalanced datasets*, volume 126, 2003.
- [10] Taeho Jo and Nathalie Japkowicz. Class imbalances versus small disjuncts. *ACM Sigkdd Explorations Newsletter*, 6(1):40–49, 2004.
- [11] Hansang Lee, Minseok Park, and Junmo Kim. Plankton classification on imbalanced large scale database via convolutional neural networks with transfer learning. In *2016 IEEE international conference on image processing (ICIP)*, pages 3713–3717. IEEE, 2016.
- [12] Samira Pouyanfar, Yudong Tao, Anup Mohan, Haiman Tian, Ahmed S Kaseb, Kent Gauen, Ryan Dailey, Sarah Aghajanzadeh, Yung-Hsiang Lu, Shu-Ching Chen, et al. Dynamic sampling in convolutional neural networks for imbalanced data classification. In *2018 IEEE conference on multimedia information processing and retrieval (MIPR)*, pages 112–117. IEEE, 2018.
- [13] Yanmin Sun, Mohamed S Kamel, Andrew KC Wong, and Yang Wang. Cost-sensitive boosting for classification of imbalanced data. *Pattern Recognition*, 40(12):3358–3378, 2007.
- [14] Robin C Geyer, Tassilo Klein, and Moin Nabi. Differentially private federated learning: A client level perspective. *arXiv preprint arXiv:1712.07557*, 2017.
- [15] Jihun Hamm, Yingjun Cao, and Mikhail Belkin. Learning privately from multiparty data. In *International Conference on Machine Learning*, pages 555–563, 2016.
- [16] Chen Huang, Yining Li, Chen Change Loy, and Xiaoou Tang. Learning deep representation for imbalanced classification. In *Proceedings of the IEEE conference on computer vision and pattern recognition*, pages 5375–5384, 2016.
- [17] Yu-Xiong Wang, Deva Ramanan, and Martial Hebert. Learning to model the tail. In *Advances in Neural Information Processing Systems*, pages 7029–7039, 2017.
- [18] Tomas Mikolov, Ilya Sutskever, Kai Chen, Greg S Corrado, and Jeff Dean. Distributed representations of words and phrases and their compositionality. In *Advances in neural information processing systems*, pages 3111–3119, 2013.
- [19] Momeng Duan, Duo Liu, Xianzhang Chen, Yujuan Tan, Jinting Ren, Lei Qiao, and Liang Liang. Astraea: Self-balancing federated learning for improving classification accuracy of mobile deep learning applications. In *2019 IEEE 37th International Conference on Computer Design (ICCD)*, pages 246–254. IEEE, 2019.
- [20] H Brendan McMahan, Eider Moore, Daniel Ramage, Seth Hampson, et al. Communication-efficient learning of deep networks from decentralized data. *arXiv preprint arXiv:1602.05629*, 2016.
- [21] Tsung-Yi Lin, Priya Goyal, Ross Girshick, Kaiming He, and Piotr Dollár. Focal loss for dense object detection. In *Proceedings of the IEEE international conference on computer vision*, pages 2980–2988, 2017.
- [22] Miroslav Kubat, Robert C Holte, and Stan Matwin. Machine learning for the detection of oil spills in satellite radar images. *Machine learning*, 30(2-3):195–215, 1998.
- [23] Haibo He and Edwardo A Garcia. Learning from imbalanced data. *IEEE Transactions on knowledge and data engineering*, 21(9):1263–1284, 2009.

[24] Shoujin Wang, Wei Liu, Jia Wu, Longbing Cao, Qinxue Meng, and Paul J Kennedy. Training deep neural networks on imbalanced data sets. In *2016 international joint conference on neural networks (IJCNN)*, pages 4368–4374. IEEE, 2016.

[25] Jesse Davis and Mark Goadrich. The relationship between precision-recall and roc curves. In *Proceedings of the 23rd international conference on Machine learning*, pages 233–240, 2006.

[26] Naeem Seliya, Taghi M Khoshgoftaar, and Jason Van Hulse. A study on the relationships of classifier performance metrics. In *2009 21st IEEE international conference on tools with artificial intelligence*, pages 59–66. IEEE, 2009.

[27] Jason Van Hulse, Taghi M Khoshgoftaar, and Amri Napolitano. Experimental perspectives on learning from imbalanced data. In *Proceedings of the 24th international conference on Machine learning*, pages 935–942, 2007.

[28] Miroslav Kubat, Stan Matwin, et al. Addressing the curse of imbalanced training sets: one-sided selection. In *Icml*, volume 97, pages 179–186. Citeseer, 1997.

[29] Nitesh V Chawla, Kevin W Bowyer, Lawrence O Hall, and W Philip Kegelmeyer. Smote: synthetic minority over-sampling technique. *Journal of artificial intelligence research*, 16: 321–357, 2002.

[30] Charles X Ling and Victor S Sheng. Cost-sensitive learning and the class imbalance problem, 2008.

[31] Yin Cui, Menglin Jia, Tsung-Yi Lin, Yang Song, and Serge Belongie. Class-balanced loss based on effective number of samples. In *Proceedings of the IEEE Conference on Computer Vision and Pattern Recognition*, pages 9268–9277, 2019.

[32] Xu-Ying Liu, Jianxin Wu, and Zhi-Hua Zhou. Exploratory undersampling for class-imbalance learning. *IEEE Transactions on Systems, Man, and Cybernetics, Part B (Cybernetics)*, 39(2): 539–550, 2008.

[33] Nitesh V Chawla, Aleksandar Lazarevic, Lawrence O Hall, and Kevin W Bowyer. Smoteboost: Improving prediction of the minority class in boosting. In *European conference on principles of data mining and knowledge discovery*, pages 107–119. Springer, 2003.

[34] Forrest N Iandola, Matthew W Moskewicz, Khalid Ashraf, and Kurt Keutzer. Firecaffe: near-linear acceleration of deep neural network training on compute clusters. In *Proceedings of the IEEE Conference on Computer Vision and Pattern Recognition*, pages 2592–2600, 2016.

[35] Hanjoo Kim, Jaehong Park, Jaehee Jang, and Sungroh Yoon. Deepspark: Spark-based deep learning supporting asynchronous updates and caffe compatibility. *arXiv preprint arXiv:1602.08191*, 3, 2016.

[36] Mu Li, David G Andersen, Jun Woo Park, Alexander J Smola, Amr Ahmed, Vanja Josifovski, James Long, Eugene J Shekita, and Bor-Yiing Su. Scaling distributed machine learning with the parameter server. In *11th {USENIX} Symposium on Operating Systems Design and Implementation ({OSDI} 14)*, pages 583–598, 2014.

[37] Pitch Patarasuk and Xin Yuan. Bandwidth optimal all-reduce algorithms for clusters of workstations. *Journal of Parallel and Distributed Computing*, 69(2):117–124, 2009.

[38] Alexander Sergeev and Mike Del Balso. Horovod: fast and easy distributed deep learning in tensorflow. *arXiv preprint arXiv:1802.05799*, 2018.

[39] Arthur Jochems, Timo M Deist, Issam El Naqa, Marc Kessler, Chuck Mayo, Jackson Reeves, Shruti Jolly, Martha Matuszak, Randall Ten Haken, Johan van Soest, et al. Developing and validating a survival prediction model for nsclc patients through distributed learning across 3 countries. *International Journal of Radiation Oncology\* Biology\* Physics*, 99(2):344–352, 2017.

[40] Arthur Jochems, Timo M Deist, Johan Van Soest, Michael Eble, Paul Bulens, Philippe Coucke, Wim Dries, Philippe Lambin, and Andre Dekker. Distributed learning: developing a predictive model based on data from multiple hospitals without data leaving the hospital—a real life proof of concept. *Radiotherapy and Oncology*, 121(3):459–467, 2016.

[41] Keith Bonawitz, Vladimir Ivanov, Ben Kreuter, Antonio Marcedone, H Brendan McMahan, Sarvar Patel, Daniel Ramage, Aaron Segal, and Karn Seth. Practical secure aggregation for privacy-preserving machine learning. In *Proceedings of the 2017 ACM SIGSAC Conference on Computer and Communications Security*, pages 1175–1191, 2017.

[42] Luca Melis, Congzheng Song, Emiliano De Cristofaro, and Vitaly Shmatikov. Exploiting unintended feature leakage in collaborative learning. *arXiv preprint arXiv:1805.04049*, 2018.

[43] Zhibo Wang, Mengkai Song, Zhifei Zhang, Yang Song, Qian Wang, and Hairong Qi. Beyond inferring class representatives: User-level privacy leakage from federated learning. In *IEEE INFOCOM 2019-IEEE Conference on Computer Communications*, pages 2512–2520. IEEE, 2019.

[44] Ligeng Zhu, Zhijian Liu, and Song Han. Deep leakage from gradients. In *Advances in Neural Information Processing Systems*, pages 14747–14756, 2019.

[45] Lixu Wang, Shichao Xu, Xiao Wang, and Qi Zhu. Eavesdrop the composition proportion of training labels in federated learning. *arXiv preprint arXiv:1910.06044*, 2019.

[46] Rangachari Anand, Kishan G Mehrotra, Chilukuri K Mohan, and Sanjay Ranka. An improved algorithm for neural network classification of imbalanced training sets. *IEEE Transactions on Neural Networks*, 4(6):962–969, 1993.

[47] Mateusz Buda, Atsuto Maki, and Maciej A Mazurowski. A systematic study of the class imbalance problem in convolutional neural networks. *Neural Networks*, 106:249–259, 2018.

[48] Jakub Konečný, H Brendan McMahan, Felix X Yu, Peter Richtárik, Ananda Theertha Suresh, and Dave Bacon. Federated learning: Strategies for improving communication efficiency. *arXiv preprint arXiv:1610.05492*, 2016.

[49] Ian J Goodfellow, Dumitru Erhan, Pierre Luc Carrier, Aaron Courville, Mehdi Mirza, Ben Hamner, Will Cukierski, Yichuan Tang, David Thaler, Dong-Hyun Lee, et al. Challenges in representation learning: A report on three machine learning contests. In *International Conference on Neural Information Processing*, pages 117–124. Springer, 2013.

[50] Kaiming He, Xiangyu Zhang, Shaoqing Ren, and Jian Sun. Deep residual learning for image recognition. In *Proceedings of the IEEE conference on computer vision and pattern recognition*, pages 770–778, 2016.